Coordination Chemistry Reviews, 92 (1988) 157–192
Elsevier Science Publishers B.V., Amsterdam – Printed in The Netherlands

REDOX CHEMISTRY OF NIOBIUM AND MOLYBDENUM PORPHYRINS

YOSHIHISA MATSUDA and YUKITO MURAKAMI

Department of Organic Synthesis, Faculty of Engineering, Kyushu University, Fukuoka, 812 (Japan)

(Received 7 September 1987)

CONTENTS

ABBREVIATIONS

acac	acetylacetonato monoanion
AcO	acetate anion
DMA	*N*,*N*′-dimethylacetamide
DMSO	dimethyl sulfoxide
Et	ethyl group
etioMe_2	α,γ-dimethyletioporphyrinato dianion
Me	methyl group
Me–THF	2-methyltetrahydrofuran
oep	octaethylporphyrinato dianion
oep–CHO	*meso*-formyloctaethylporphyrinato dianion
oep–NCO	*meso*-isocyanatooctaethylporphyrinato dianion
oep–NH_2	*meso*-aminooctaethylporphyrinato dianion
omp	octamethylporphyrinato dianion
por	porphyrinato dianion

0010-8545/88/$12.60

tdbp	tetra(3,5-di-*t*-butylphenyl)porphyrinato dianion
THF	tetrahydrofuran
tmtp	tetra-*m*-tolylporphyrinato dianion
tpp	tetraphenylporphyrinato dianion
tpXpp	tetra-(*p*-substituted phenyl)porphyrinato dianion
tptp	tetra-*p*-tolylporphyrinato dianion

A. INTRODUCTION

Natural metalloporphyrins have been extensively investigated from the viewpoint of elucidating their physiological functions. A large number of porphyrin complexes containing the first series transition metals, in most cases the later half of the series, have been prepared, and their structures, redox behavior and photochemistry investigated as an extension of studies on natural porphyrin complexes. The porphyrin complexes containing transition metals of the second and third series have also been studied in relation to the biochemical functions of iron porphyrins. However, a relatively smaller number of studies have been reported on the chemistry of metallo-

TABLE 1

Niobium(IV) porphyrins and visible absorption data

Complex	Solvent	Wavelength ($\epsilon \times 10^{-3}$) (nm)					Ref.
Nb(O)(por)							17, 19, 20, 22
Nb(O)(oep)	THF	403(100)	455(7)	538(10)	577(14)		20
NB(O)(oep)	THF	403(100)		538(10)	577(14)		17
Nb(O)(oep)	THF	407(220)		538(13)	575(18)		19
Nb(O)(oep^{-})	THF	408(88)	414(88)	613(18)	665(9)	806(7)	19
Nb(O)(oep^{2-})	THF	414(45)	455(30)	538(11)	582(15)	769(6)	19
Nb(O)(tpp)	PhCN	430(278)	555(16)	596(5)			19
Nb(O)(tpp)	PhCN	440(99)	718(7)				19
Nb(O)(tpp^{2-})	PhCN	442(6.9)	559(12)	605(15)			19
Nb(O)(tptp)	THF	428(195)	462(9)	557(15)	558(3.5)		20
Nb(O)(tptp)	THF	428(195)		557(15)	558(3.8)		17
$Nb(X)_2(por)$							16, 17
$Nb(Cl)_2$(tpp)	THF	427					17
$Nb(Cl)_2$(tmtp)	THF	438					17
$Nb(Cl)_2$(tptp)	THF	438					17
$Nb(Br)_2$(tpp)	THF	438					17
$Nb(Br)_2$(tmtp)	THF	438					17
$[Nb(O)(F)(por)]^{-}$							17, 20

porphyrins containing the earlier transition metals of the second and third series. The significance of these studies has been rather diverse as compared with that of studies on the first series transition metal complexes. Niobium

TABLE 2

Niobium(V) porphyrins and visible absorption data

Complex	Solvent	Wavelength ($\epsilon \times 10^{-3}$) (nm)					Ref.
Nb(O)(OAc)(por)							8–10, 15, 17, 19, 20, 22
Nb(O)(OAc)(omp)							9
Nb(O)(OAc)(oep)	THF	410(127)	522(6)	538(10)	565(15)	583(10)	19
Nb(O)(OAc)(oep)	THF	410(140)	520(6)	540(10)	565(17)	585(11)	20
Nb(O)(OAc)(tpp)	PhCN	430(297)	533(8)	555(12)			19
Nb(O)(OAc)(tpp)	THF	425(300)	534(10)	555(15)	601(1)		20
Nb(O)(OAc)(tptp)	THF	428(272)	535(10)	554(15)	602(2)		20
Nb(O)(X)(por)							4, 5, 14, 40, 64
Nb(O)(F)(omp)	CH_2Cl_2	400(100)	528(9)	556(17)			14
Nb(O)(F)(oep)	Toluene	404(195)	530(9.8)	568(30)			14
Nb(O)(F)(oep)	CH_2Cl_2	402(170)	531(10.5)	569(27.5)			5
Nb(O)(F)(tpp)	Toluene	420(316)	538(18)				14
Nb(O)(F)(tptp)	Toluene	423(400)	541(23)				14
Nb(O)(I_3)(oep)	CH_2Cl_2	342(22.8)	406(88)	535(6.7)	569(13.7)		64
{Nb(O)(I_3)(oep)}$_2$	CH_2Cl_2	396(100)	533(7.6)	571(15.1)			5
{Nb(O)(I)(oep)}$_2$	CH_2Cl_2	399(85.1)	530(7.2)	570(13.2)			5
Nb(X)$_3$(por)							4, 5, 16, 17
Nb(F)$_3$(oep)	CH_2Cl_2	403(186)	532(8.3)	569(24.0)			4, 5
Nb(O)(OR)(HOR)(por)							23
Nb(O)(OO)(por)							23, 24
Nb(X)$_2$(OO)(por)							16
{Nb(por)}$_2$O$_3$							4, 8–10, 12, 13, 18, 23, 64
{Nb(oep)}$_2$O$_3$		402	530	570			8
{Nb(oep)}$_2$O$_3$	Benzene	406(107)	442(7.8)	571(16.6)			64
{Nb(oep)}$_2$O$_3$	THF	399(210)	538(16)	570(34)			18
{Nb(tpp)}$_2$O$_3$		419	530	570			8

and molybdenum porphyrins have been studied in more detail relative to other porphyrin complexes of the second and third series earlier transition metals.

The preparation of molybdenum porphyrins was reported in 1970 by Srivastava and Fleischer [1,2]. Buchler and his coworkers have reported several porphyrin complexes of the earlier transition metals [3–7]. Since this preparative work was reported, studies on the niobium and molybdenum porphyrins have been developed from the following viewpoints:

(1) Preparation of complexes possessing less familiar structures, and clarification of the nature of coordination in such complexes. There is a tendency for the early transition metals in high valence states to form seven or more coordinate bonds.

(2) The construction of catalytic systems exhibiting functions similar to those of cytochrome P450. Niobium and molybdenum porphyrins readily form stable oxo structures with the central metals in the +5 valence state. The oxygen atom at the axial coordination site was expected to be transferred to substrates such as olefins in a manner similar to that observed for high valent oxoiron or oxomanganese porphyrins.

(3) To control softness of the central metals in the porphyrin complexes. Preparation of the porphyrin complexes with a very soft central metal was proposed by using lower valent niobium or molybdenum porphyrins. Such complexes are expected to have a high affinity for acetylene and molecular nitrogen, so that good catalysts for nitrogen fixation may be developed.

TABLE 3

Molybdenum(II) porphyrins and visible absorption data

Complex	Solvent	Wavelength ($\epsilon \times 10^{-3}$) (nm)					Ref.
$Mo(NO)_2$(tptp)	CH_2Cl_2	390(513)	468(407)	551(36)	586(18)	622(8)	46
Mo(NO)(OMe)(tptp)	CH_2Cl_2	425(871)	551(36)	586(18)	622(8)		46
Mo(PhC≡CPh)(oep)	Toluene	406	534	564	574		47
Mo(PhC≡CPh)(tptp)	Benzene	426(158)	544(9.5)	624(2.3)			45
$[Mo(oep)]_2$	Toluene	356(52.5)	384(72)	439(36)	534(10.2)	574(5.8)	47
$[Mo(etioMe_2)]_2$	Toluene	394(331) 600(1.6)	432(14.1)	442(10.2)	484(4.4)	548(3.0)	47
$[Mo(oep-CHO)]_2$	Toluene	388(53.7)	441(25.1)	544(6.9)	585(4.8)		47
$[Mo(oep-NH_2)]_2$	Toluene	411(141)	476(26.3)	546(11.5)			47
$[Mo(oep-NCO)]_2$	Toluene	393	420	440	488		47
[Mo(oep–CHO)]-[Mo(oep)]	Toluene	364(10.7) 578(1.5)	386(14.5)	409(9.8)	442(6.6)	539(2.1)	47

TABLE 4

Molybdenum(IV) porphyrins and visible absorption data

Complex	Solvent	Temp. (°C)	Wavelength ($\epsilon \times 10^{-3}$) (nm)					Ref.
Mo(O)(por)								3, 5, 6, 31, 34, 40, 41, 44, 47, 50–53, 58
Mo(O)(oep)	CH_2Cl_2		412(182)	540(12.0)	578(20.9)			3, 5
Mo(O)(oep)	Toluene		413(213)	540(10.7)	578(22.9)	644(0.9)		47
Mo(O)(tpp)	CH_2Cl_2		431(110)	514(2)	554(10.3)			53
Mo(O)(tpp)	Me–THF	25	427(360)	555(23)	588(5.8)			44
Mo(O)(tpp)	CH_2Cl_2	25	429(295)	511(3.79)	553(17.2)	590(3.4)	640(1.2)	51
Mo(O)(tptp)	CH_2Cl_2		431(1100)	514(20)	554(103)	592(13)		31
Mo(L)$_2$(por)								31, 42, 43, 47
Mo(Cl)$_2$(oep)	CH_2Cl_2		354(57)	406(143)	530(30)	574(24)		42
Mo(Cl)$_2$(oep)	Toluene		369	400	490			47
Mo(Cl)$_2$(tptp)	CH_2Cl_2		360(42)	429(105)	488(28)	550(10)		31, 42
Mo(PhN$_2$)(tptp)	Benzene		431(447)	554(27.5)	593(13.5)	635(10.2)		43
[Mo(O)(L$^-$)(por)]$^-$								43
[Mo(O)(F)(tpp)]$^-$	Me–THF	−196	447(670)	577(19)	617(16)			43
[Mo(O)(NCS)(tpp)]$^-$	Me–THF	−196	448(1080)	583(21)	625(18)			43
[Mo(O)(Cl)(tpp)]$^-$	Me–THF	−196	456(350)	588(22)	631(21)			43
[Mo(O)(Br)(tpp)]$^-$	Me–THF	−196	464(230)	592(18)	638(22)			43
Mo(O)(L)(por)								2, 40, 44
Mo(O)(Me–THF)(tpp)	Me–THF	−196	422(590)	572(41)	610(40)			44
Mo(O)(Me–THF)(tpp)	Me–THF	−72	437(410)	566(23)	606(11)			44
Mo(O)(DMSO)(tpp)	CH_2Cl_2	−72	445(343)	573(14.7)	614(8.5)			40
Mo(O)(py)$_2$(tpp)	Pyridine		379(55)	385(56)	412(37)	434(44)	456(24)	2
			540(8.2)	572(88)	650(4.8)			

TABLE 5

Molybdenum(V) porphyrins and visible absorption data

Complex	Solvent	Temp. (°C)	Wavelength ($\epsilon \times 10^{-3}$) (nm)					Ref.
Mo(O)(OR)(por)								1, 2, 4–7, 22, 25–27, 29, 30, 48–53, 56, 58, 60, 61, 63, 65
Mo(O)(OMe)(oep)	CH_2Cl_2		443(87.1)	512(3.5)	562(15.1)	595(10.0)		6
Mo(O)(OMe)(oep)	$CHCl_3$		447(67.2)	563(14.4)	595(9)			27
Mo(O)(OMe)(tpp)	CH_2Cl_2		454(170)	540(3.8)	581(15.7)	621(10.8)		25
Mo(O)(OMe)(tpp)	CH_2Cl_2		454(170)	540(3.8)	583(10.8)			53
Mo(O)(OMe)(tpp)	CH_2Cl_2 [a]	25	455(146)	538(4.31)	583(15.3)	623(10.3)	725(0.2)	22
Mo(O)(OEt)(tpp)	CH_2Cl_2	25	454(158)	582(15.1)	622(10.4)			29, 30
Mo(O)(OEt)(tpp)	CH_2Cl_2		453(182)	540(3.5)	581(15.9)	620(10.9)		25
Mo(O)(OEt)(tpp)	$CHCl_3$		457(128)	583(14.2)	625(9.5)			27
Mo(O)(O^{i}Pr)(tpp)	CH_2Cl_2		453(196)	537(3.4)	580(16.2)	619(11.1)		25
Mo(O)(O^{t}Bu)(tpp)	CH_2Cl_2		451(224)	536(3.3)	578(17.6)	617(12.3)		25
Mo(O)($OC_6H_{10}OH$)(tpp)	Benzene		456(177)	584(22.4)	624(16.1)			60
Mo(O)(OPh)(oep)	Benzene		454(69.2)	573(14.1)	606(8.1)			7
Mo(O)(OAc)(oep)	CH_2Cl_2		444(49.0)	592(8.1)	620(3.9)			5
Mo(O)(OAc)(tpp)	CH_2Cl_2 [b]	25	485(52.6)	610(9.41)	653(7.63)			51
Mo(O)(OH)(tpp)	CH_2Cl_2		464(90)	593(10.8)	635(8.4)			25
Mo(O)(OH)(tpp)	Solid		463	590	632			25
Mo(O)(X^-)(por)								1, 2, 5, 6, 25–30, 35, 40, 44, 51, 60, 61, 65
Mo(O)(F)(oep)	CH_2Cl_2		458(45.7)	576(8.91)	610(5.0)			5,6
Mo(O)(F)(tpp)	CH_2Cl_2	25	463(97.1)	592(13.0)	635(10.4)			30

Mo(O)(F)(tpp)	Me–THF	25	463(95.5)	587(12.1)	627(9.9)		44
Mo(O)(F)(tpp)	Me–THF	−196	460(95)	475(11)	591(17)	633(21)	44
Mo(O)(Cl)(oep)	CH_2Cl_2		500(25.7)	607(10.5)			5
Mo(O)(Cl)(oep)	$CHCl_3$		497(23.3)	607(1.03)			27
Mo(O)(Cl)(tpp)	CH_2Cl_2	25	500(41.7)	627(8.5)	674(9.6)		30
Mo(O)(Cl)(tpp)	CH_2Cl_2		504(41)	632(8.4)	678(9.2)		26
Mo(O)(Cl)(tpp)	CH_2Cl_2	25	503(39.0)	630(8.4)	676(9.7)	722(2.3)	51
Mo(O)(Cl)(tpp)	CH_2Cl_2		498(43)	628(8.6)	674(9.3)		25
Mo(O)(Cl)(tpp)	CH_2Cl_2	25	499(41.9)	626(8.5)	673(9)		29
Mo(O)(Cl)(tpp)	$CHCl_3$		504(44)	631(8.9)	676(9.45)		1, 2
Mo(O)(Cl)(tpp)	Me–THF	25	493(40.3)	623(8.3)	670(9.3)		44
Mo(O)(Cl)(tpp)	Me–THF	−196	499(42)	516(43)	630(10)	675(16)	44
Mo(O)(Br)(tpp)	CH_2Cl_2	25	508(34.5)	638(7.1)	686(8.6)		30
Mo(O)(Br)(tpp)	CH_2Cl_2	25	481(48.3)	602(9.2)	648(6.9)		29
Mo(O)(Br)(tpp)	CS_2	25	521(44.6)	642(9.3)	689(12.0)		35
Mo(O)(Br)(tpp)	Benzene	25	514(40.6)	640(8.5)	687(11.1)		35
Mo(O)(Br)(tpp)	THF	25	513(39.6)	639(8.4)	686(11.1)		35
Mo(O)(Br)(tpp)	Me–THF	25	508(32.7)	635(6.7)	688(8.6)		44
Mo(O)(Br)(tpp)	Me–THF	−196	507(36)	527(37)	642(8.6)	689(1.4)	44
Mo(O)(L$^-$)(por)							5, 29, 30, 35, 40, 44, 53, 54, 57
Mo(O)(BF_4)(tpp)	CH_2Cl_2	25	463(98.2)	591(13.5)	634(10.9)		30
Mo(O)(N_3)(tpp)	CH_2Cl_2	25	490(43.4)	616(8.1)	662(8.3)		30
Mo(O)(NCO)(tpp)	CH_2Cl_2	25	488(46.6)	617(8.5)	664(8.6)		30
Mo(O)(SCN)(oep)	CH_2Cl_2	25	492(26.9)	602(10.0)	633(4.7)		5
Mo(O)(NCS)(tpp)	CH_2Cl_2	25	493(45.5)	622(9.1)	667(9.3)		30
Mo(O)(NCS)(tpp)	CH_2Cl_2	25	496(43.5)	623(8.9)	668(8.7)		29
Mo(O)(NCS)(tpp)	CS_2	25	500(63.2)	624(11.6)	670(11.7)		35

TABLE 5 (continued)

Complex	Solvent	Temp. (°C)	Wavelength ($\epsilon \times 10^{-3}$) (nm)					Ref.
Mo(O)(NCS)(tpp)	Benzene	25	498(54.1)	624(10.1)	669(10.4)			35
Mo(O)(NCS)(tpp)	THF	25	495(50.5)	622(10.1)	668(10.7)			35
Mo(O)(NCS)(tpp)	Me–THF	25	492(47.6)	621(9.4)	667(9.8)			44
Mo(O)(NCS)(tpp)	Me–THF	−196	496(51)	512(50)	625(11)	671(16)		44
Mo(O)(ClO_4)(tpp)	$C_2H_4Cl_2$		489	607	655			57
Mo(O)(ClO_4)(tpp)	CH_2Cl_2		480(49)	616(16)	664(15)			53
[Mo(O)(L)(por)]$^+X^-$								34, 35
Mo(O)(DMSO)(tpp)Br	CH_2Cl_2 [c]	25	477(60)	604(10)	648(9)			34, 35
Mo(O)(DMSO)(tpp)Cl	CH_2Cl_2 [c]	25	478(70)	605(13)	651(9)			35
Mo(O)(DMSO)(tpp)NCS	CH_2Cl_2 [c]	25	477(68)	604(13)	651(10)			35
Mo(O)(MeOH)(tpp)Br	CH_2Cl_2		478(54)	600(10)	645(8)			34
Mo(O)(OO)(por)								40, 56, 60
Mo(O)(OO^{t}Bu)(tpp)	Benzene		344(39)	480(54)	607(11.3)	652(8.9)		60
Mo(O)(OOH)(tpp)	Dioxane		342(37.3)	484(54)	609(10.5)	653(8.2)		56
[Mo(O)(O_2^{2-})(tpp)]$^-$	CH_2Cl_2 [d]	−72	445(35.3)	565(9.5)	586(12.9)	604(7.8)	635(14.7)	40
{Mo(O)(por)}$_2$O								4, 12, 13, 25, 26, 32, 38, 51, 53, 62
{Mo(O)(tpp)}$_2$O	Benzene		410(36)	444(59)	583(3.5)	617(4.2)	667(3.3)	25
{Mo(O)(tpp)}$_2$O	Solid		445	590	622	674		25

[a] Containing 2% (v/v) MeOH. [b] Containing 2% (v/v) AcOH. [c] Containing DMSO (less than 2.5×10^{-2} M). [d] Containing 2% (v/v) DMSO.

TABLE 6

Molybdenum(VI) porphyrins and visible absorption data

Complex	Solvent	Wavelength ($\epsilon \times 10^{-3}$) (nm)				Ref.
Mo(O_2)$_2$(por)						36, 38, 53, 55
Mo(O_2)$_2$(tptp)	CH_2Cl_2	444(250)	576(11)	616(20)		36
Mo(O_2)$_2$(tptp)	Benzene	445(465)	533(4.2)	574(19.4)	615(23.8)	38
Mo(O_2)$_2$(tmtp)	CH_2Cl_2	444(165)	532(4)	572(25)	613(30)	53
Mo(O)$_2$(por)						37–39, 53, 56, 57, 60, 61
Mo(O)$_2$(tpp)	CH_2Cl_2	425(214)	487(4.6)	535(15.2)	562(11)	53
Mo(O)$_2$(tptp)	Benzene	425(216)	487(4.6)	535(15.2)	562(11)	38

(4) Preparation of one-dimensional polymer complexes with "stacked planar molecules". These metal ions have larger ionic radii compared with those of the first series transition metal ions in the same oxidation states and are known to form metal–metal multiple bonds in their lower oxidation states.

In addition, the authors have recently found that photoreduction of niobium and molybdenum porphyrins led to the reductive activation of

TABLE 7

Structures of niobium and molybdenum porphyrins confirmed by X-ray diffraction study

Central metal	Complex	Coordination number and structure [a]	Ref.
Nb(IV)	$Nb_2(tpp)_2O_3$	7 *cis* (op) Staggerd [b]	9, 11
	$Nb_2(tpp)_2O_3$	7 *cis* (op) Slipped [b]	12, 13
	Nb(O)(OAc)(tpp)	7 *cis* (op)	9, 10
	Nb(O)(F)(oep)	6 *cis* (op)	14
Mo(II)	Mo(tptp)(PhC≡CPh)	6 *cis* (op)	45
	Mo(tptp)($NO)_2$	6 *cis* (op)	46
	Mo(tptp)(NO)(MeOH)	6 *trans* (Oh)	46
Mo(IV)	Mo(O)(tptp)	5 Square pyramid (op)	31
	Mo($Cl)_2$(tptp)	6 *trans* (Oh)	31, 42
	Mo($N_2Ph)_2$(tptp)	6 *trans* (Oh)	43
Mo(V)	Mo(O)(Cl)(tpp)	6 *trans* (Oh)	28
	[Mo(O)(tpp)]$_2$O	6 *trans* (Oh)	12, 13
Mo(VI)	Mo($O)_2$(tptp)	6 *cis* (op)	37
	Mo($O_2)_2$(tptp)	8 *trans*	36

[a] *cis* and *trans*, the axial coordination geometry with respect to each other; Oh, metal located at the center of octahedron; op, metal located out of the plane formed by four nitrogen atoms. [b] Configuration of two porphyrin ligands.

molecular oxygen that induced exclusive epoxidation of olefins. The development of reductive activation processes for small molecules is expected, with the complexes reduced upon light irradiation.

Since these various aspects are concerned with the oxidation states of the central metal ions, this article reviews the redox chemistry of niobium and molybdenum porphyrins which are listed in Tables 1–6 together with their solution visible absorption data. X-ray diffraction studies are summarized in Table 7.

B. PREPARATION AND CHEMICAL REDUCTION AND OXIDATION OF PENTAVALENT NIOBIUM AND MOLYBDENUM COMPLEXES

(i) Niobium complexes

The preparation of niobium porphyrins, an oxohalo complex, $[Nb^{V}(O)(X)(oep)]$, and a trifluoroniobium complex of oep, $[Nb^{V}(O)(F)(oep)]$, was first reported by Buchler and coworkers [4,5]. The most stable valence state of niobium in the porphyrin complexes is +5; known niobium(V) species are mostly oxo complexes such as tri-μ-oxo dimers **1**, oxoacetato complexes **2** and oxohalo complexes **3**. Trihalo complexes **4** are also known.

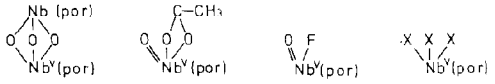

1 2 3 4

To incorporate the niobium into the porphyrin ring, the following method has been adopted. $NbCl_5$ and a porphyrin are reluxed in benzonitrile for several hours [4,5,8], and the solvent is removed by distillation under reduced pressure. The product is extracted with chloroform or dichloromethane. The solution is treated with alkaline water to afford the corresponding tri-μ-oxo dimer. Complexes with other axial ligands are obtained by ligand-exchange reactions with the appropriate acid or salts. The dimer complexes were presumed to have a μ-oxo structure with octahedral geometry similar to that observed for the molybdenum dimer complexes.

Molecular structures of four oxoniobium(V) porphyrins, an oxoacetato complex, Nb(O)(OAc)(tpp) [9,12], two types of tri-μ-oxo complexes, $[\{Nb(tpp)\}_2O_3]$ [9,11–13], and an oxofluoro complex, Nb(O)(F)(oep) [14], were confirmed by X-ray diffraction measurements. All these complexes have a *cis* configuration with respect to the axial ligands, indicating a strong *cis* configuration tendency of the d^0 ion; the axial ligands in these complexes are located on the same side with respect to the equatorial porphyrin ligand. The niobium–oxo bond is highly stabilized and cannot be cleaved by

chemical reduction. Therefore oxoniobium(IV) porphyrins are obtained by chemical reduction as described later. It is therefore more convenient to use complexes having no oxo ligand as precursors for the preparation of complexes in different metal oxidation states because it is difficult to remove the oxo ligand by chemical reduction. For this purpose, trihalo complexes are preferable as precursors. A trifluoro complex, $Nb^{V}(F)_3(oep)$, has been reported for the first time by Buchler and Rohbock [4,5] on treatment of $[\{Nb^{V}(oep)\}_2O_3]$ with HF in toluene. Later, trichloro and tribromo niobium complexes of several porphyrins were prepared by treatment with anhydrous hydrogen halides in aromatic solvents [15–17]. Although molecular structures for these complexes have not been clarified by X-ray diffraction measurements, the *cis* configuration of these halogen ligands has been suggested in the light of IR and NMR data as well as the strong *cis* configuration tendency of the d^0 ion [4].

Since niobium(V) has no *d* electrons, oxidation of niobium(V) porphyrins may take place at the porphyrin moiety. Chemical oxidation of niobium(V) porphyrins has not been reported, while electrochemical oxidation was attempted by Kadish and coworkers [18,19]. However, reduction with several reductants has been reported [16,17,20]. Chemical reduction of oxoniobium(V) complexes of several porphyrins with reductants such as zinc amalgam gives the corresponding oxoniobium(IV) complex (eqn. (1)) [20]:

$$Nb^{V}(O)(OAc)(por) \xrightarrow[THF]{Zn/Hg} Nb^{IV}(O)(por) \quad (1)$$

Aluminum powder also reduced oxoacetato and tri-μ-oxo complexes to afford the corresponding oxoniobium(IV) complexes [21].

The stretching Nb=O vibration is shifted by about 100 cm^{-1} to higher frequency upon reduction (Tables 8–12). A similar shift was observed for molybdenum complexes forming penta-coordinate complexes upon reduction. Although X-ray structural data are not available, oxoniobium(IV) complexes are presumed to have a penta-coordinate structure with a slight displacement of the niobium atom from the porphyrin plane.

The tetravalent niobium has one *d* electron and niobium(IV) porphyrins show characteristic ESR signals (Fig. 1). Spin Hamiltonian parameters for

TABLE 8

Nb=O stretching frequencies for niobium(IV) porphyrins

Complex	Medium	$\nu_{Nb=O}$ (cm^{-1})	Ref.
Nb(O)(oep)	Nujol	1020	17, 20
Nb(O)(tpp)	Nujol	1020	17, 20
Nb(O)(tptp)	Nujol	1020	17, 20

TABLE 9

Nb=O stretching frequencies for niobium(V) porphyrins [a]

Complex	Medium	$\nu_{Nb=O}$ (cm^{-1})			Ref.
Nb(O)(OAc)(omp)	CsI	900	608	698	9
Nb(O)(OAc)(oep)	CsI	900	610	692	9
Nb(O)(OAc)(oep)		900		700	8
Nb(O)(OAc)(oep)		900			20
Nb(O)(OAc)(tpp)		900		700	8
Nb(O)(OAc)(tpp)	CsI	900	582	652	9
Nb(O)(OAc)(tptp)	CsI	910	580	700	30
Nb(O)(F)(omp)	CsI	910	545(Nb–F)		14
Nb(O)(F)(oep)	KBr	900	540(Nb–F)		4, 5
Nb(O)(F)(oep)	CsI	910	540(Nb–F)		14
Nb(O)(F)(tpp)	CsI	910	555(Nb–F)		14
Nb(O)(F)(tptp)	CsI	910	550(Nb–F)		14
$Nb(O)(I)_3$(oep)	KBr		470	353	64
$Nb(F)_3$(oep)	KBr		598(Nb–F)		4, 5
Nb(O)(acac)(tpp)	Nujol	898			15
$\{Nb(oep)\}_2O_3$	CsI	702			9
$\{Nb(oep)\}_2O_3$	KBr	690			4, 5
$\{Nb(oep)\}_2O_3$	KBr	690	742	785	64
$\{Nb(tpp)\}_2O_3$	KBr	515			12
$\{Nb(tpp)\}_2O_3$	CsI	662			9
$\{Nb(tptp)\}_2O_3$	CsI	718			9

[a] Unassigned absorption bands were presumed to be due to the coordination bonds.

niobium(IV) complexes are summarized in Table 13. The oxoniobium(IV) complexes show large hyperfine splitting constants, indicating that an odd electron is located primarily on the niobium atom [22].

Guilard and coworkers examined hexa-coordinate oxoniobium(IV) complexes of porphyrins [17,20] and reported that products obtained by the amalgam reduction of oxofluoroniobium(V) complexes showed a set of spin

TABLE 10

Mo=O stretching frequencies for molybdenum(IV) porphyrins

Complex	Medium	$\nu_{Mo=O}$ (cm^{-1})		Ref.
Mo(O)(oep)	KBr	965		3
Mo(O)(oep)	KBr	952		7
Mo(O)(tptp)	Nujol	970		31
Mo(O)(tptp)	CH_2Cl_2	980		39
$Mo(Cl)_2$(oep)			268(Mo–Cl)	42
$Mo(Cl)_2$(tptp)			330(Mo–Cl)	31, 42

TABLE 11

Mo=O stretching frequencies for molybdenum(V) porphyrins

Complex	Medium	$\nu_{Mo=O}$ (cm^{-1})			Ref.
[Mo(O)(O_2^{2-})(tpp)] 18-Cr-6-K	KBr	903	521(Mo–O)	490(Mo–O)	40
Mo(O)(OMe)(oep)	KBr	896	442(Mo–O)		5, 7
Mo(O)(OMe)(oep)	KBr	910 (Raman)			63
Mo(O)(OMe)(tpp)	KBr	905	475(Mo–O)		25, 26
Mo(O)(OEt)(tpp)	KBr	897			26
Mo(O)(OEt)(tpp)	Nujol	904			29
Mo(O)(OEt)(tpp)	KBr	901	520(Mo–O)		25
Mo(O)(OEt)(tpp)	Nujol	904			30
Mo(O)(O^{i}Pr)(tpp)	KBr	901			26
Mo(O)(O^{i}Pr)(tpp)	KBr	904			25
Mo(O)(O^{t}Bu)(tpp)	KBr	902	518(Mo–O)		25
Mo(O)(O^{t}Bu)(tpp)	KBr	900			26
Mo(O)(OPh)(oep)	KBr	910			5, 7
Mo(O)(OAc)(oep)	KBr	928			5
Mo(O)(F)(oep)	KBr	926	465(Mo–F)		5
Mo(O)(F)(oep)	KBr	938	485(Mo–F)		6
Mo(O)(F)(tpp)	Nujol	938			30
Mo(O)(Cl)(oep)	KBr	926			5
Mo(O)(Cl)(tpp)	Nujol	935			29, 30
Mo(O)(Cl)(tpp)	KBr, Nujol	937	242(Mo–Cl/Aerosil)		28
Mo(O)(Cl)(tpp)	CH_2Cl_2	934			25
Mo(O)(Br)(tpp)	Nujol	937			29, 30
Mo(O)(BF_4)(tpp)	Nujol	940			30
Mo(O)(N_3)(tpp)	Nujol	935			30
Mo(O)(NCO)(tpp)	Nujol	940			30
Mo(O)(SCN)(oep)	KBr	936			5
Mo(O)(NCS)(tpp)	Nujol	950			30
Mo(O)(NCS)(tpp)	Nujol	953			29
Mo(O)(OH)(tpp)	KBr	923			25
{Mo(O)(oep)}$_2$O	KBr		630(M–O–M)		4, 5
{Mo(O)(tpp)}$_2$O	KBr	905	615(M–O–M)	565(M–O–M)	12
{Mo(O)(tpp)}$_2$O	KBr	900	648(M–O–M)	615(M–O–M)	26

TABLE 12

Mo=O stretching frequencies for molybdenum(VI) porphyrins [a]

Complex	Medium	$\nu_{Mo=O}$ (cm^{-1})			Ref.
Mo(O)$_2$(tptp)	KBr	900	866		38
Mo(^{18}O)$_2$(tptp)	KBr	900	892	832	38
Mo(O$_2$)$_2$(tptp)	KBr		970(O–O)		38

[a] Unassigned absorption bands were presumed to be due to the coordination bonds.

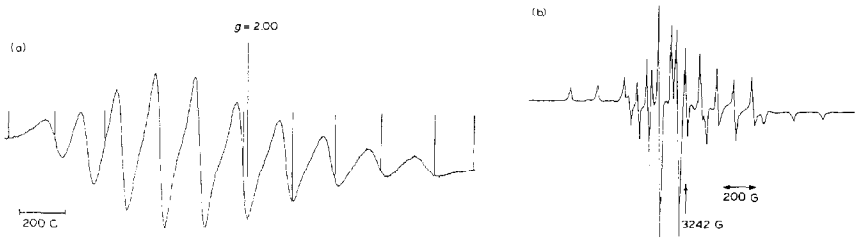

Fig. 1. ESR spectra for niobium(IV) porphyrins: (a) $Nb^{IV}(O)$(tptp) in benzene at room temperature [62]; (b) $Nb^{IV}(Cl)_2$(tptp) in THF at 77 K [16].

Hamiltonian parameters different from those for oxo complexes (Table 13). They obtained the same species during the electrochemical reduction of a niobium(V) porphyrin only when PF_6^- was added to the solution [16]. The ESR signals were attributed to oxofluoroniobium(IV) complex anions, $[Nb(O)(F)(por)]^-$. The oxofluoroniobium(IV) complexes have smaller g and A values relative to the corresponding oxoniobium(IV) complexes, indicating that the oxofluoro complexes assume an "elongated octahedral" geometry. In other words, the axial ligand field in the oxofluorocomplexes must be weaker than that in the oxo complexes.

TABLE 13

Spin Hamiltonian parameters for niobium(IV) porphyrins

Complex	Medium	Temp. [a]	g_{av}	$g_{\parallel}$	$g_{\perp}$	A_{av} [b]	$A_{\parallel}$ [b]	$A_{\perp}$ [b]	Ref.
Nb(O)(oep)	THF	RT	1.967			166			17
Nb(O)(tpp)	THF	RT	1.968			165			17
Nb(O)(tpp)	CH_2Cl_2	RT	1.96			175			22
Nb(O)(tptp)	THF	RT	1.969			165			17
$Nb(O)(F)(oep)^-$	THF	RT	1.942			131			20
$Nb(O)(F)(tpp)^-$	THF	RT	1.938			131			20
$Nb(O)(F)(tptp)^-$	THF	RT	1.943			131			20
$Nb(Cl)_2$(tpp)	THF	RT	1.962			143			16, 17
$Nb(Cl)_2$(tmtp)	THF	RT	1.962			148			16, 17
$Nb(Cl)_2$(tptp)	THF	RT	1.962			148			16, 17
$Nb(Br)_2$(tpp)	THF	RT	1.962			147			16, 17
$Nb(Br)_2$(tmtp)	THF	RT	1.962			147			16, 17
Nb(O)(oep)	Toluene	LNT		1.934	1.972		−246	−132	17
Nb(O)(tptp)	Toluene	LNT		1.947	1.972		−235	−127	17
$Nb(Cl)_2$(tptp)	Toluene	LNT		1.942	1.965		−224	−112	16
$Nb(Br)_2(OO)$(tpp)	THF	RT	2.002			10.8			16
Nb(O)(OO)(tpp)	Benzene	RT	2.011			5.08			23, 24

[a] RT, room temperature; LNT, liquid nitrogen temperature. [b] A in 10^{-4} cm^{-1}.

TABLE 14

Spin Hamiltonian parameters for molybdenum(V) porphyrins

Complex	Solvent	Temp. [a]	g_{av}	A_{Nav} [b]	A_{Moav} [b]	Ref.
Mo(NO)(MeOh)(tptp)	Powder	RT	1.968		−99.66	46
Mo(O)(OMe)(tpp)	CH_2Cl_2	RT	1.969	2.30	46.0	25
Mo(O)(OEt)(tpp)	CH_2Cl_2	RT	1.969	2.30	46.0	25
Mo(O)(OEt)(tpp)	CH_2Cl_2	RT	1.967	2.21	45.5	29
Mo(O)(OEt)(tpp)	CH_2Cl_2	RT	1.964	2.34	45.2	27
Mo(O)(OEt)(tpp)	CH_2Cl_2	LNT	1.964(parallel)		72.9	27
			1.960(perpendicular)		31.2	
Mo(O)(OEt)(tdbp)	Benzene	RT	1.969	2.28		62
Mo(O)(O'Pr)(tpp)	CH_2Cl_2	RT	1.969	2.30	46.0	25
Mo(O)(O'Bu)(tpp)	CH_2Cl_2	RT	1.969	2.30	46.0	25
Mo(O)(OAc)(oep)	CH_2Cl_2	RT	1.962	2.34	44.0	27
Mo(O)(OAc)(oep)	CH_2Cl_2	LNT	1.964(parallel)		70.8	27
Mo(O)(OH)(tpp)		RT	1.974	2.30		49
Mo(O)(OH)(tpp)	CH_2Cl_2	RT	1.968	2.30	45.9	25
Mo(O)(OH)(tdbp)	Benzene	RT	1.967	2.42		62
Mo(O)(NCS)(tpp)	CH_2Cl_2	RT	1.967	2.26	44.3	29
Mo(O)(Cl)(oep)	CH_2Cl_2	RT	1.962	2.39	44.0	27
MO(O)(Cl)(tpp)	CH_2Cl_2	RT	1.967	2.17	45.5	29
Mo(O)(Cl)(tpp)	CH_2Cl_2	RT	1.965	2.29	45.9	25
Mo(O)(Br)(tpp)	CH_2Cl_2	RT	1.967	2.33	44.7	29
		−150 °C	1.961 (perpendicular)			40
Mo(O)(OO^{2-})(tpp)	CH_2Cl_2	−20 °C	1.971	2.54		40
Mo(O)(OO^{2-})(tpp)	CH_2Cl_2	−150 °C	1.953			40
			1.969			
			2.004			
$[Mo(O_2)_2(tmtp)]^-$	CH_2Cl_2	RT	1.980			55

[a] RT, room temperature; LNT, liquid nitrogen temperature. [b] A in 10^{-4} cm^{-1}.

The trihalo complexes can be reduced with zinc amalgam to afford complexes having a composition $Nb(X)_2(por)$ (eqn. (2)):

$$Nb^{V}(X)_3(por) \xrightarrow[THF]{Zn/Hg} Nb^{IV}(X)_2(por) \quad (2)$$

Richard and Guilard observed ESR spectra for those complexes with axially symmetric spin Hamiltonian parameters [16,17] (Table 13). They presumed that these complexes assume an octahedral geometry with some tetragonal distortion. This means that one halogen must move from one side of the porphyrin plane to the other during the reaction, or that intermolecular transfer of the halogen atom takes place.

The niobium(IV) species are not stable under aerobic conditions. The niobium(IV) complexes are subject to facile reoxidation by atmospheric

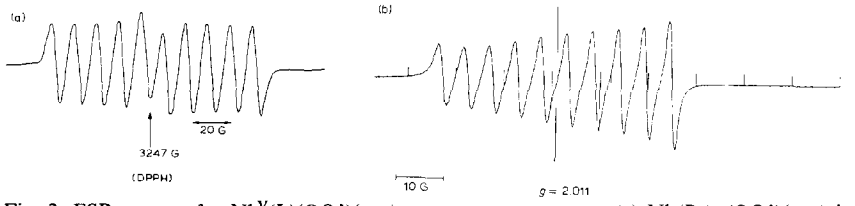

Fig. 2. ESR spectra for $Nb^{V}(L)(OO^{\cdot})(por)$ at room temperature: (a) $Nb(Br)_2(OO^{\cdot})(tpp)$ in THF [16]; (b) NB(O)$(OO^{\cdot})$(tptp) in benzene [23,24].

oxygen in the presence of a catalytic amount of water to the tri-μ-oxo dimer (eqn. (3)):

$$2\ Nb(O)(por) + 1/2\ O_2 \longrightarrow (por)Nb\begin{matrix}\diagup O \diagdown \\ -O- \\ \diagdown O \diagup\end{matrix}Nb(por) \qquad (3)$$

Richard and Guilard investigated the reoxidation process for $Nb^{IV}(X)_2$ (por), where X = Br, and por denotes oep, tpp, tptp or tmtp. They found ESR-active species which show ten hyperfine lines, suggesting that the niobium nucleus is included in the oxidized species. However, the hyperfine splitting by the niobium nuclear spin is much smaller than that observed for oxoniobium(IV) porphyrins. The spin Hamiltonian parameters were estimated to be $g = 2.002$ and $A = 10.8 \times 10^{-4}$ cm^{-1} (Fig. 2(a)). These species are relatively stable under anhydrous conditions. The ESR signal was attributed to superoxide complexes, $Nb^{V}(X)_2(O_2^{\cdot})$(por) [16]. They observed the ν_{O-O} mode at 1220 cm^{-1} for samples prepared by different methods. Matsuda et al. found another ESR-active species having a smaller A_{Nb} value [23,24] during photoreaction of $Nb(tptp)_2O_3$ in benzene (Fig. 2(b)) and assigned to it the structure Nb(O)$(OO^{\cdot})$(tptp). The latter superoxide complex has been reported to be highly reactive, as mentioned later.

(ii) Molybdenum complexes

The molybdenum complexes so far reported are summarized in Tables 3–6. The valence state ranges from +2 to +6. Complexes having an oxidation state other than +5 have been derived from the corresponding pentavalent molybdenum complexes.

Molybdenum porphyrins were prepared first by Srivastava and Fleischer [1,2] from $Mo(CO)_6$ and H_2tpp in refluxing or heated benzonitrile. The complexes were presumed to have an octahedral structure, and an axial ligand such as Cl^-, OH^- or OOH^- was expected to be located at a position *trans* to the oxo ligand. Characterization of the latter two complexes (with

OH^- and OOH^-), however, was insufficient [25,26]. Buchler and coworkers prepared several oxomolybdenum complexes of oep from $MoCl_2$ or $Mo(acac)_3$ [3–7].

Most porphyrin complexes of pentavalent molybdenum have been prepared by the reaction of molybdenum hexacarbonyl or molybdenum(II) dichloride with porphyrins in heated organic solvents having high boiling points. The complexes obtained under aerobic conditions were confirmed to have the oxomolybdenum(V) structure [6,27,28].

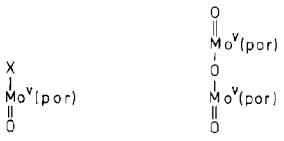

5 6

Most oxomolybdenum(V) complexes are known to have one monodentate monoanion as a ligand at the sixth coordination site, *trans* to the oxo ligand **5**, to form neutral complexes. The axial ligand placed *trans* to the oxo group can be readily replaced with other ligands [25–27,29,30]. Purification treatments, such as recrystallization and liquid chromatography, with chloroform lead to the formation of an oxoalkoxo complex upon ligand exchange, with an alcohol added to the solvent as a stabilizer. Complexes with a large variety of axial ligands have been reported (Tables 3–6). Oxohalo complexes have been obtained by the reaction of oxoalkoxo complexes in aromatic solvents with hydrogen halides under strictly anhydrous conditions [6,13]. The oxomolybdenum complexes are subject to hydrolysis by a trace amount of water in solvents, and the oxohalo complexes are more sensitive to water than the oxoalkoxo complexes. Hydrolysis leads to the formation of the corresponding oxohydroxo complexes (eqn. (4)). The oxohydroxo complex readily gives the μ-oxo dimer **6** upon dehydration (eqn. (5)).

$$Mo(O)(X)(por) + H_2O \rightarrow Mo(O)(OH)(por) + HX \quad (4)$$

$$2Mo(O)(OH)(por) \rightarrow (por)Mo(O)\text{–}O\text{–}Mo(O)(por) + H_2O \quad (5)$$

The μ-oxo dimers of *meso*-tetraphenylporphyrin and tetratolylporphyrin are so poorly soluble in organic solvents that the oxochloro complexes upon treatment in organic solvents with water immediately precipitate the μ-oxo dimers. An oxochloro complex, Mo(O)(Cl)(tpp) [28], and a μ-oxo dimer, $[\{Mo(O)(tpp)\}_2O]$ [12,13], are the only oxomolybdenum(V) complexes whose molecular structures have been confirmed by X-ray diffraction studies. The coordination polyhedron for both complexes is a tetragonally distorted

octahedron, and the molybdenum atom deviates towards an oxo group or a terminal oxo ligand from the plane formed by the four nitrogen atoms. The oxoalkoxo complexes have not been subjected to structural analysis by means of X-ray diffraction. On the basis of their IR data Buchler et al. [6] and Rohbock [5] assigned the *trans* distorted octahedral structure to these complexes.

The pentavalent molybdenum has one *d* electron and oxomolybdenum(V) complexes are ESR active. Mononuclear molybdenum(V) complexes in solution show ESR spectra composed of two superimposed signals. One signal is attributed to species containing $I = 0$ molybdenum nuclei, ^{94,96,98,100}Mo (Figs. 3(b) and 3(c)), and consists of a symmetric nine-hyperfine-line pattern due to four coordinating nitrogen nuclei. The other signal is due to complexes containing $I \neq 0$ molybdenum nuclei, ^{95,97}Mo, and consists of six hyperfine lines with almost symmetric spacing with a slight second-order effect (Fig. 3(a)). The μ-oxo dimers show large spin–spin interactions which have been elucidated in terms of a localized dipole model [32]. The spin Hamiltonian parameters are summarized in Table 14. As mentioned above, the oxoalkoxo and oxohalo complexes are subject to hydrolysis. Special care is therefore required to prevent hydrolysis or other ligand exchange in their ESR measurements [25,33].

The acetate anion can generally act both as a monodentate and a bidentate ligand when it is coordinated to molybdenum(V). Oxoacetato complexes have been prepared [6], and the acetato ligand is plausibly located at the site opposite to the oxo ligand. Matsuda et al. presumed that the acetato ligand is coordinated as a bidentate ligand [22].

The ligand exchange of oxomolybdenum(V) complexes with neutral ligands has also been reported (eqn. (6)):

$$[\mathrm{Mo(O)(X)(por)}] + \mathrm{L} \rightarrow [\mathrm{Mo(O)(L)(por)}]^{+}(\mathrm{X})^{-} \qquad (6)$$

Imamura et al. observed spectrophotometrically the exchange equilibria between halogen or NCS^- and DMSO or MeOH [34,35]. These monocationic species (eqn. (6)) were stable only in solution.

7

8

Two different coordination geometries have been reported for the complexes containing molybdenum(VI), whereas all known complexes of oxomolybdenum(V) have tetragonally distorted octahedral geometry. The bisperoxo complexes, **7** [36], have one type of geometry and the dioxo complexes, **8** [37] have another. The bisperoxomolybdenum(VI) porphyrin,

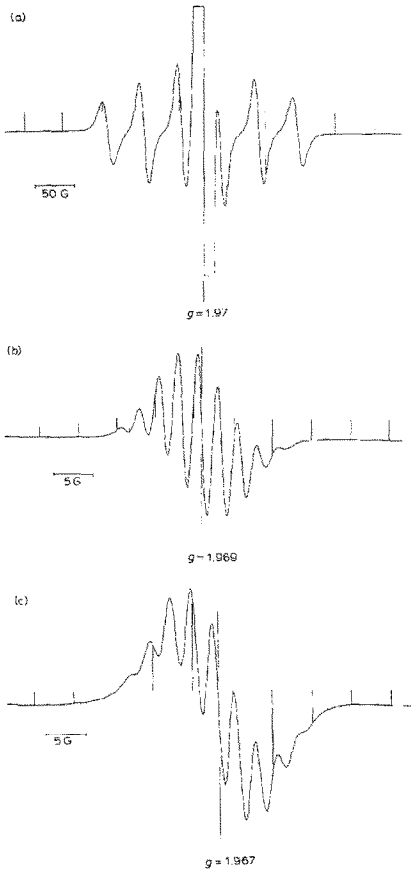

Fig. 3. ESR spectra for Mo(O)(OR)(tdbp) in benzene at room temperature. (a) Whole spectrum for Mo(O)(OEt)(tdbp). An intense line at the center is attributed to the complexes containing $I = 0$ molybdenum, while six hyperfine lines are due to the $I \neq 0$ molybdenum. (b) Central portion of the spectrum (due to complexes of the $I = 0$ molybdenum). Nine symmetric hyperfine lines are due to the coordinated nitrogen nuclei. (c) Central intense signal for Mo(O)(OH)(tdbp).

$Mo(O_2)_2$(tptp), has two peroxo ligands located on opposite sides of the porphyrin plane and has $O_2N_4O_2$ geometry in which each peroxo ligand is bidentate. However, the *cis*-dioxo molybdenum complex has two oxo ligands on the same side with respect to the porphyrin plane [36].

$Mo^{VI}(O_2)_2$(por) was prepared by Chevrier et al. [36] by oxidation of Mo^{V}(O)(OH)(por) in dichloromethane with H_2O_2. An X-ray diffraction

study was carried out. While the bisperoxo complexes are thermally stable, Ledon and Bonnet found that the bisperoxo complexes give the corresponding *cis*-dioxo complexes upon anaerobic irradiation with visible light [38] (eqn. (7)):

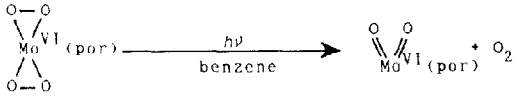

(7)

Complexes obtained on photoreaction have the *cis*-dioxo structure, confirmed by X-ray diffraction measurements [39]. The same authors reported that *cis*-dioxo complexes can transfer an oxygen atom to triphenylphosphine [39].

Porphyrin complexes of tetravalent molybdenum, except for the oxomolybdenum porphyrins, $Mo^{IV}(O)(por)$, were prepared by a two-step reaction from the oxomolybdenum(V) complexes: preparation of oxomolybdenum complexes, $Mo^{IV}(O)(por)$, and the subsequent replacement of the oxo ligand by ligand exchange.

Oxomolybdenum(IV) complexes were prepared by chemical reduction with amalgamated zinc as reported by Weiss and coworkers [31] (eqn. (8)):

$$Mo(O)(Cl)(por) \xrightarrow{Zn/Hg} Mo(O)(por) \tag{8}$$

The oxomolybdenum(V) complexes, Mo(O)(X)(por), release a ligand placed *trans* to the oxo ligand, affording the corresponding oxomolybdenum(IV) complexes, Mo(O)(por), upon reduction with zinc amalgam. The thermal reduction of oxomolybdenum(V) complexes takes place during sublimation under reduced pressure as reported by Buchler et al. [3] (eqn. (9)):

$$Mo^{V}(O)(oep) \xrightarrow[10^{-4}\ \text{Torr}]{250\,^{\circ}C} Mo^{IV}(O)(oep) \tag{9}$$

Imamura and coworkers carried out the reduction of Mo(O)(X)(tpp) ($X = Cl^-$, Br^- or NCS^-) with KO_2 which was dissolved in an aprotic solvent containing a crown ether [34,40,41] (eqns. (10) and (11)):

$$Mo^{V}(O)(X)(tpp) + O_2 \rightarrow [Mo^{V}(O)(OO^{\cdot})(tpp)] + X^- \tag{10}$$

$$[Mo^{V}(O)(OO^{\cdot})(tpp)] \rightarrow Mo^{IV}(O)(tpp) + O_2 \tag{11}$$

A superoxide complex was reduced at lower temperatures with the superoxide ion to afford the corresponding oxoperoxo complex, $[Mo^{V}(O)(O_2^{2-})(por)]$.

As regards other preparative methods for porphyrin complexes of tetravalent molybdenum, Fleischer and Srivastava reduced Mo(O)(OH)(tptp) with hydrazine in pyridine to afford $Mo(O)(py)_2(tpp)$ [2]. The detailed characterization of the product, however, was not given.

A tetragonal pyramid structure has been confirmed for an oxomolybdenum(IV) complex, $Mo^{IV}(O)(tpp)$, by X-ray diffraction measurements [31]. The Mo=O stretching vibration is shifted toward higher frequency relative to that of the corresponding molybdenum(V) complexes (Tables 10, 11).

The oxo ligand in oxomolybdenum(IV) porphyrins can be replaced upon ligand exchange with the chloro ligand, while it is hardly replaced in the case of oxomolybdenum(V) porphyrins. Weiss and coworkers prepared $Mo(Cl)_2(tptp)$ upon treatment of Mo(O)(tptp) with HCl in benzene under strictly anhydrous and deoxygenated conditions [31,42]. The dichloro complex exhibits an octahedral coordination structure with tetragonal distortion. A bis(diphenyldiazo) complex has been prepared via the reaction of $Mo(Cl)_2(tptp)$ with phenylhydrazine [43]. The product has octahedral geometry.

Imamura et al. studied other reduction processes with the oxomolybdenum(V) complexes [44]. When a 2-methyltetrahydrofuran solution of an oxomolybdenum complex, Mo(O)(X)(tpp) ($X = NCS^-$, F^-, Cl^- or Br^-) was irradiated with γ-rays at 77 K, the solvent was ionized to a cation and an electron. The electron thus formed in the rigid glass matrix was trapped by the complex, resulting in the corresponding molybdenum(IV) species. Because the complexes are surrounded by a rigid solvent glass at 77 K, the axial ligand cannot diffuse out of the reaction sphere after the reduction at the central metal takes place. The axial ligand, therefore, is forced to coordinate to the central metal. The Soret and α and β bands of oxomolybdenum(V) complexes are shifted to shorter wavelength upon reduction, affording penta-coordinate oxomolybdenum(IV) complexes (Tables 4, 5). The spectral pattern for the constrained complexes is quite similar to those observed for the reduced penta-coordinate species. The extent of the blue shift is smaller for the constrained complexes than that observed for the penta-coordinate species. In the light of these observations and the fact that the constrained complexes are ESR silent, the complexes were formulated as $[Mo(O)(tptp)(X^-)]^-$ [35]. These authors reported preparation of the oxomolybdenum porphyrins with additional neutral ligands [35,40]. These complexes were formulated as $Mo^{IV}(O)(tpp)(L)$, where L denotes a neutral ligand such as DMSO or 2-methyltetrahydrofuran. The visible absorption spectra for these complexes are similar to those observed for the penta-coordinate ones and stable only below 0 °C. A detailed structural characterization of these complexes needs to be carried out in the future.

Molybdenum porphyrins in lower metal oxidation states have also been prepared. Weiss and coworkers reported the syntheses of Mo(tptp)(PhC≡CPh) [45], $Mo(tptp)(NO)_2$ [46], and $Mo(tptp)(NO)(CH_2OH)$ [46] by reduction of dichloromolybdenum(IV) porphyrin.

Collman and Woo studied the preparation of molybdenum(II) dimer complexes without any bridging ligand by thermal decomposition of the diphenyl acetylene complexes of the molybdenum(II) porphyrin [45] in connection with the development of one-dimensional polymer complexes [47].

C. ELECTROCHEMISTRY

(i) Niobium porphyrins

The electrolysis of niobium porphyrins was reported first in 1980 by Guilard et al. [20]. They prepared oxoacetatoniobium complexes of oep, tpp and tptp and examined them by means of the rotating electrode and cyclic voltammetry in THF. Three reduction potentials were observed for each complex. The first reduction potentials of Nb(O)(OAc)(por) were observed at -1.1 V, -0.92 V and -0.90 V for por of oep, tpp and tptp respectively. These potentials were assigned to reduction at the central metal, Nb(V)/Nb(IV), accompanied by cleavage of the Nb–OAc bond. The assignment was confirmed by visible absorption and ESR measurements. They followed the electrolysis by ESR and found a new signal with smaller g and A_{Nb} values only when PF_6^- was added to the solution as a counter-ion of the supporting electrolyte. They attributed the signal to $[Nb^{IV}(O)(F^-)(por)]^-$ which was formed upon coordination of the fluoro ligand to the pentacoordinate complexes. A similar ESR signal was observed also upon chemical reduction with zinc amalgam. The second and third reduction potentials for each complex were assigned to reduction of the porphyrin ring because the redox reactions at these potentials are reversible and the potential separations satisfy Fuhrhop's relation [48].

Matsuda et al. carried out cyclic voltammetry and controlled potential electrolysis for Nb(O)OAc)(tpp) in dichloromethane. They observed reduction potentials at -0.89, -1.05 and -1.41 V vs. the standard calomel electrode (SCE). The peak potentials for the first two steps showed cathodic shifts of about 0.3 V upon addition of pyridine, while the peak potential for the third reduction process remained unchanged. On the basis of variations in the reduction potentials caused by changes in axial coordination structure, they assigned the couples at -0.89 V and -1.05 V to reduction of niobium(V) to niobium(IV) and niobium(IV) to niobium(III) respectively [22] (Scheme 1). The assignments were confirmed by ESR measurements during controlled potential bulk electrolysis. During the electrolysis at -0.92 V, an ESR signal due to $Nb^{IV}(O)$(tptp) ($g = 1.96$; $A = 175 \times 10^{-4}$ cm^{-1}) was observed. The intensity of the ESR signal increased with progress of the electrolysis, while the ESR signal decreased when the applied poten-

TABLE 15

Redox potentials for niobium porphyrins

Complex	Medium	Temp. [a] (°C)	E [b] (V(SCE))					Ref.
Nb(O)(OAc)(oep)	THF	RT	1.10		−1.10*	−1.25	−1.66	17, 20
Nb(O)(OAc)(oep)	THF	22	1.06	−0.1*	−1.07*	−1.15	−1.52	19
Nb(O)(OAc)(oep)	THF	−75	1.07	0.00*	−1.20*	−1.17	−1.53	19
Nb(O)(OAc)(oep)	CH_2Cl_2	22	0.98	0.05*	−1.18*	−1.24	−1.71	19
Nb(O)(OAc)(oep)	CH_2Cl_2	−75	0.98	0.11*	−1.23*	−1.20	−1.67	19
Nb(O)(OAc)(oep)	PhCN	22	0.98	0.05*	−1.16*	−1.25	−1.71	19
Nb(O)(OAc)(oep)	"PrCN	22	1.01	−0.02*	−1.16*	−1.24	−1.70	19
Nb(O)(OAc)(oep)	"PrCN	−75	1.00	0.00*	−1.24*	−1.21	−1.66	19
Nb(O)(oep)	THF	RT		0.55*		−1.20	−1.60	17, 20
Nb(O)(OAc)(tpp)	THF	RT	1.24		−0.92*	−1.03	−1.45	17, 20
Nb(O)(OAc)(tpp)	CH_2Cl_2	25			−0.89*	−1.05*	−1.41	22
Nb(O)(OAc)(tpp)	THF	22		0.10*	−0.88*	−0.93	−1.33	19
Nb(O)(OAc)(tpp)	CH_2Cl_2	22	1.21	0.17*	−0.94*	−1.00	−1.38	19
Nb(O)(OAc)(tpp)	CH_2Cl_2	−76	1.21	0.20*	−0.96*	−0.95	−1.33	19
Nb(O)(OAc)(tpp)	PhCN	22	1.23	0.16*	−0.90*	−0.97	−1.41	19
Nb(O)(OAc)(tpp)	Pyridine	22		0.02*	−0.89*	−0.95	−1.36	19
Nb(O)(OAc)(tpp)	DMSO	22		−0.10*	−0.80*	−0.87	−1.27	19
Nb(O)(tpp)	THF	RT				−0.96	−1.44	17, 20
Nb(O)(OAc)(tptp)	THF	RT	1.38		−0.90*	−1.01	−1.48	17, 20
Nb(O)(OAc)(tptp)	THF	22		0.14*	−0.92*	−0.97	−1.37	19
Nb(O)(OAc)(tptp)	CH_2Cl_2	22	1.15	0.20*	−0.98*	−1.02	−1.41	19
Nb(O)(OAc)(tptp)	PhCN	22	1.19	0.17*	−0.95*	−1.01	−1.46	19
Nb(O)(tptp)	THF	RT				−0.91	−1.42	17, 20
Nb(O)(acac)(tpp)	THF	22		0.14*	−1.09*	−0.91	−1.33	19
Nb(O)(acac)(tpp)	THF	−60	1.17		−1.12*	−0.94	−1.32	19
Nb(O)(acac)(tpp)	CH_2Cl_2	22	1.03	0.18*	−1.18*	−1.00	−1.39	19
Nb(O)(acac)(tpp)	CH_2Cl_2	−74	1.05	0.27*	−1.14*	−0.95	−1.32	1
$Nb(O)(F)(oep)^-$	THF	RT		0.96	−1.48	−0.95	−1.70	20
$Nb(O)(F)(tpp)^-$	THF	RT		1.14	−0.69	−1.18		20
$Nb(O)(F)(tptp)^-$	THF	RT		1.09	−0.71	−1.2		20
$\{Nb(oep)\}_2O_3$	THF	22		0.78	−1.29	−1.63	−1.92	18
$\{Nb(oep)\}_2O_3$	THF	−78	1.12	0.72	−1.30	−1.63	−1.93	18
$\{Nb(oep)\}_2O_3$	CH_2Cl_2	22	1.09	0.63	−1.40	−1.86		18
$\{Nb(oep)\}_2O_3$	CH_2Cl_2	−40	1.20	0.63	−1.39	−1.86		18
$\{Nb(oep)\}_2O_3$	"PrCN	22	1.07	0.68	−1.38	−1.80	−2.09	18
$\{Nb(oep)\}_2O_3$	"PrCN	−50	1.04	0.68	−1.37	−1.80	−2.13	18
$\{Nb(oep)\}_2O_3$	PhCN	22	1.10	0.66	−1.43	−1.87		18
$\{Nb(oep)\}_2O_3$	Pyridine	22		0.72	−1.41	−1.84		18
$\{Nb(tpp)\}_2O_3$	CH_2Cl_2	−24			−1.27	−1.50	−1.73	22
$\{Nb(tptp)\}_2O_3$	THF			1.13	−1.18	−1.41	−1.66	18
$\{Nb(tptp)\}_2O_3$	CH_2Cl_2		1.20	0.89	−1.28	−1.53	−1.75	18
$\{Nb(tptp)\}_2O_3$	PhCN		1.22	0.94	−1.21	−1.50	−1.73	18

[a] RT, room temperature. [b] *, redox potential with respect to central metal.

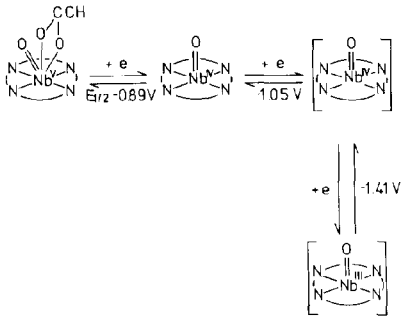

Scheme 1

TABLE 16

Redox potentials for molybdenum porphyrins

Complex	Medium	Temp. [a] (°C)	E [b] (V(SCE))				Ref.
Mo(O)(OH)(oep)	BuCN	20	1.43				48
Mo(O)(OH)(oep)	DMSO	20	−0.21*		−1.30	−1.72	48
Mo(O)(OH)(tpp)	CH_2Cl_2	RT	0.11	0.11*	−1.31		49
Mo(O)(OH)(tpp)	DMSO	RT		0.01*	−0.98	−1.34	49
Mo(O)(OH)(tpp)	Pyridine	RT		0.11*	−0.80	−1.30	−1.44	49
Mo(O)(OH)(tpp)	DMA	RT		0.02*			49
Mo(O)(tpp)	CH_2Cl_2		1.49	0.02*		−1.13	−1.48	53
Mo(O)(ClO_4)(tpp)	CH_2Cl_2		1.48	0.02*		−1.13	−1.48	53
Mo(O)(OH)(tpp)	CH_2Cl_2		1.48	−0.10*		−1.13	−1.48	53
Mo(O)(OMe)(tpp)	CH_2Cl_2		1.48	−0.83*		−1.13	−1.48	53
[Mo(O)(DMSO)-(tpp)] (OMe)	CH_2Cl_2		1.48	−0.03*		−1.14	−1.49	53
Mo(O)(tpp)	CH_2Cl_2			0.02*		−1.15	−1.53	52
Mo(O)(OMe)(tpp)	CH_2Cl_2			0.2*	−0.89*	−1.15	−1.50	52
Mo(O)(NCS)(tpXpp)								
X = −OMe	DMSO	RT		0.0*		−1.02	−1.40	54
−Me	DMSO	RT		0.013*		−1.01	−1.39	54
−H	DMSO	RT		0.03*		−0.99	−1.36	54
−F	DMSO	RT		0.05*		−0.96	−1.32	54
−Cl	DMSO	RT		0.07*		−0.94	−1.29	54
−Br	DMSO	RT		0.07*		−0.94	−1.29	54
Mo(O)(OMe)(tpp)	CH_2Cl_2	26		−0.73*		−1.13	−1.49	50
Mo(O)(OMe)(tpp)	CH_2Cl_2	25		−0.74*		−1.14	−1.49	51
Mo(O)(OAc)(tpp)	CH_2Cl_2	25		−0.04*		−1.11	−1.51	51
Mo(O)(Cl)(tpp)	CH_2Cl_2	25		−0.06*		−1.11	−1.50	51
$Mo(O_2)_2$(tmtp)	CH_2Cl_2		1.18	−0.09*	−1.46*			53, 55
$Mo(O)_2$(tpp)	$C_2H_4Cl_2$		1.49	1.25	−0.96*			53, 56, 57
$Mo(O)_2$(tptp)	CH_2Cl_2				0.92*	−1.13	−1.48	53

[a] RT, room temperature. [b] *, redox potential with respect to central metal.

tial was raised to −1.1 V. An ESR signal due to a radical species was observed upon reduction at −1.46 V, indicating that the first and second electrons occupied the same orbital and the third electron was unpaired in the porphyrin π-orbital.

The redox behavior of the acetatoniobium porphyrins was examined by Anderson et al. [19]. They observed similar redox behavior for both acetato and acetylacetonato complexes. These complexes are concerned with two oxidation and three reduction processes; the latter processes are similar to those reported by Matsuda et al. [22]. The first oxidation peak in the cyclic voltammetry was not observed in the first scan but in the second and subsequent scans. This process is assigned to reoxidation of the oxoniobium(IV) complexes. The second oxidation process was attributed to oxidation of the porphyrin ring (Scheme 2). Since the pentavalent niobium does not have *d* electrons, the oxidation of niobium(V) porphyrins takes place at the porphyrin ring as mentioned earlier. One irreversible reduction at −0.9 V (SCE) and two reversible reduction processes at −1.0 and −1.4 V (SCE) were reported for the oep complex of oxoacetatoniobium(V) in THF. The corresponding potentials were observed at slightly more positive potentials for the tpp and tptp complexes relative to those for the oep complexes. These potentials were assigned on the basis of spectroelectrochemical observations. The first reduction took place at the central metal to afford primarily $[Nb^{IV}(O)(OAc^-)(por)]^-$ on the time scale of cyclic voltammetry, and the reduction was followed by elimination of the acetate anion. The second and third reduction processes were assigned to addition of electrons to the porphyrin ring without any structural change (Scheme 2). The products in such steps were $[Nb^{IV}(O)(por)]$, $[Nb^{IV}(O)(por^-)]^-$, and $[Nb^{IV}(O)(por^{2-})]^{2-}$. The product assignment for the second reduction step does not agree with that by Matsuda et al. [22]. The formation of

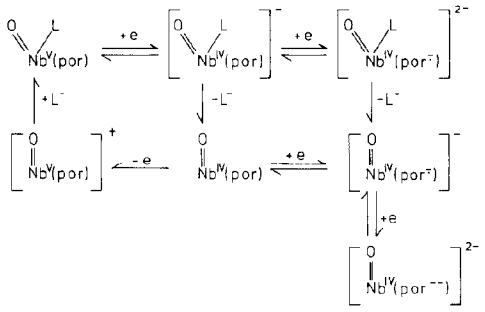

Scheme 2

$[Nb^{IV}(O)(por^{-})]^{-}$, which was claimed for the second reduction step, was based on the following observations: (i) the second and third reduction steps were not accompanied by a change in the molecular structure; (ii) the Soret band is weakened upon reduction along with a slight shift of the band to longer wavelength and evolution of a new band in a longer-wavelength region. The assignment means that the two odd electrons are located separately in *d* and π orbitals in the first two reduction steps. A decrease in intensity of the ESR signal due to the niobium(IV) species was observed upon reduction at -1.08 V (SCE) for the tpp complex. Under these circumstances, the ESR signal may decrease in intensity by forming a singlet ground state or enhancing the relaxation. They claimed that the third electron was added to a porphyrin orbital. There should be three electrons added, and they assume that one is added to a niobium *d* orbital and the other two to porphyrin π orbitals. This electron configuration cannot provide a reasonable explanation for the anion radical nature of the three-electron reduction product characterized by its specific visible absorption and the strong ESR signal. Detailed discussions are required for identification of the reduction sites. Both research groups consistently concluded that the first reduction took place at the niobium site.

The electrochemical reduction of tri-μ-oxo dimers of niobium porphyrins has been investigated by Matsuda et al. [22]. They reported three redox couples in the ranges between -1.23 and -1.30, -1.44 and -1.56, and -1.66 and -1.80 V (SCE) without assignment of the reduction sites. The electrochemistry of two tri-μ-oxo dimers, $[\{Nb(oep)\}_2O_3]$ and $[\{Nb(tptp)\}_2O_3]$, was investigated in several solvents by Anderson et al. [18]. In the positive potential region, the oep complex showed three oxidation potentials, 0.66, 1.10 and 1.43 V (SCE). Each of these processes was a one-electron oxidation, and the first two steps were reversible. The first two oxidation steps were assigned to the formation of $[\{Nb(oep)\}_2O_3]^{+}$ and $[\{Nb(oep)\}_2O_3]^{2+}$. These assignments were confirmed by bulk oxidation at 0.8 and 1.3 V (SCE) followed by ESR. Both of the tri-μ-oxo dimer complexes showed three redox pairs in the negative potential region in accord with the results obtained by Matsuda et al. [22]. Anderson et al. assigned reduction steps observed at -1.29 V (SCE), -1.63 V (SCE) and -1.92 V (SCE) to the reactions given by eqn. (12), eqn. (13) and eqn. (14) respectively:

$$[\{Nb(oep)\}_2O_3] \rightarrow [\{Nb(oep)\}_2O_3]^{-} \tag{12}$$

$$[\{Nb(oep)\}_2O_3]^{-} \rightarrow [\{Nb(oep)\}_2O_3]^{2-} \tag{13}$$

$$[\{Nb(oep)\}_2O_3]^{2-} \rightarrow [\{Nb(oep)\}_2O_3]^{3-} \tag{14}$$

All these redox pairs were reversible in nature, and there was no structural change upon reduction on the time scale of cyclic voltammetry. They also examined the bulk reduction by visible absorption and ESR measurements to clarify the reduction sites. The bulk electrolysis of $[\{Nb(oep)\}_2O_3]$ at -1.34 V (SCE) resulted in generation of an ESR signal due to a radical species. The first electron was incorporated into a π orbital of the porphyrin ring. They continued reduction at -1.5 V (SCE) and observed two ESR signals. The first was of a radical nature, and the second was due to the tetravelent niobium in the second reduction step. They suggested for the overall three-electron process that the first and second electrons were added to the porphyrin π orbitals of the dimer complex separately, and that the complex was decomposed to monomer species after the second reduction of the dimer, and converted into $[Nb^{IV}(O)(oep^{2-})]^{2-}$. The final product, showing an ESR signal characteristic of niobium(IV), was assigned to $[Nb^{IV}(O)(oep^{2-})]^{2-}$. In the case of the oep complex, formation of the monomer species was observed at room temperature even on the cyclic voltammetry time scale. More careful examination is required for identification of the reduction sites.

(ii) Molybdenum porphyrins

The electrochemistry of molybdenum porphyrins was investigated in 1973 by Fuhrhop et al. [48]. They observed the Mo(V)/Mo(IV) redox potential of Mo(OH)(O)(oep) in DMSO at -0.12 V (SCE). The detailed characterization of the complex was not reported by the authors. In 1975, Newton and Davis [49] reported the redox potentials for Mo(OH)(O)(tpp) in several solvents. They claimed that the first electron was added to the molybdenum and the second and third electrons to π orbitals of the porphyrin ligand. The oxohydroxomolybdenum porphyrin used in these studies was not sufficiently characterized [25].

Matsuda et al. investigated the electrochemical redox behavior of Mo(O)(OMe)(tpp) using cyclic voltammetry and controlled potential electrolysis, and followed by ESR measurements [50,51]. They observed three reduction processes and one oxidation process. The first reduction was reported to occur at the central metal, Mo(V)/Mo(IV), while the second and third reductions occur at the porphyrin ring system. $Mo^{V}(O)(OMe)(tpp)$ was reduced at -0.84 V (SCE) in dichloromethane to afford $Mo^{IV}(O)(tpp)$. The latter species was reoxidized at 0 V (SCE) to give $Mo^{V}(O)(OMe)(tpp)$ and $Mo^{V}(Cl)(O)(por)$, where the chloride anion was supplied from tetrabutylammonium chloride as supporting electrolyte [50]. The potential for reduction at the central metal, Mo(V)/Mo(IV), varied as the polarity of the

axial coordination bond was changed, while the reduction potentials related to the porphyrin moiety were hardly affected [51]. They also showed that Mo(O)(tpp) was reduced to a molybdenum(III) species in a potential range more negative than that for the two one-electron reduction steps at the porphyrin moiety (Scheme 3).

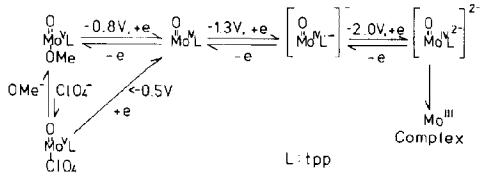

Scheme 3

Kadish and coworkers investigated the redox behavior of $Mo^{V}(O)(X)(tpp)$ and $Mo^{IV}(O)(tpp)$ [52,53]. Three and two reduction steps were observed for $Mo^{V}(O)(X)(tpp)$ and $Mo^{IV}(O)(tpp)$ respectively. The first reduction of $Mo^{V}(O)(X)(tpp)$ was an irreversible one-electron process, while the others were reversible one-electron processes. The first reduction process was assigned to a reduction at the central metal, Mo(V)/Mo(IV) and the subsequent two processes were due to reduction at the porphyrin ligand [53]. While Kadish et al. proposed in their earlier work rather complicated reaction pathways to elucidate the bulk electrolysis [52], their data apparently indicated that $Mo^{V}(O)(OMe)(tpp)$ was reduced to $Mo^{IV}(O)(tpp)$, accompanied by cleavage of the Mo–OMe bond. The results are essentially the same as those reported by Matsuda et al. [50,51].

Topich and Berger reported a relation between the reduction potential and the electronic property of the substituents at the *meso* phenyl groups of tetraarylporphyrins [54]. They prepared porphyrins having *para*-substituted phenyl groups at the *meso* positions, H_2tpXpp, where X is CH_3O–, CH_3–, H–, Cl– or Br–. Mo(O)(NCS)(tpXpp) showed three reduction potentials in the ranges between 0.068 and 0 V, −0.0938 and −1.018 V and −1.285 and −430 V for Mo(V)/Mo(IV), por/por$^-$ and por$^-$/por^{2-} respectively. All three potentials were shifted toward positive potential upon substitution with an electron-withdrawing group. The potential related to the reduction of the central metal was less affected relative to that for reduction of the porphyrin ring.

The redox chemistry of the diperoxomolybdenum(VI) complex of tptp (see 7) was reported in 1983 by Kadish and coworkers [53,55]. They observed three reversible one-electron reduction steps at 1.18, −0.09 and −1.46 V (SCE), which were assigned to the following reactions:

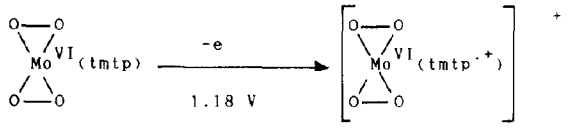

(15)

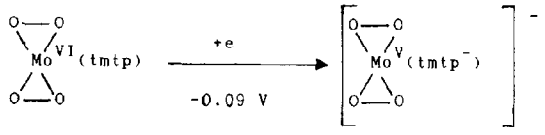

(16)

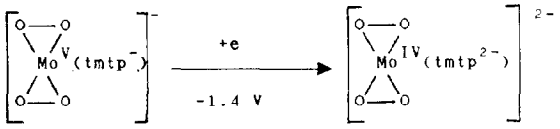

(17)

On the cyclic voltammetry time scale the complexes do not seem to undergo structural changes because all these redox pairs are reversible. The products obtained by one-electron oxidation and reduction were cation radical and anion species containing the pentavalent molybdenum respectively, as confirmed by bulk electrolysis monitored by visible absorption and ESR measurements. These species, generated by bulk electrolysis, are presumably identical with those generated during cyclic voltammetry. The second reduction process, however, gave rise to demetallation during bulk reduction.

Other complexes containing hexavalent molybdenum are *cis*-dioxomolybdenum porphyrins, **8**. The electrochemistry of these complexes is more complicated than that of the diperoxo complexes mentioned above [53,56,57]. A *cis*-dioxo complex, $Mo(O)_2(tpp)$, showed two oxidation steps in cyclic voltammetry at 1.25 and 1.49 V(SCE). The former was irreversible, while the latter was reversible. The product obtained by bulk oxidation was $Mo^{V}(O)(ClO_4)(tpp)$, confirmed by visible absorption measurements carried out during the oxidation. The first oxidation potential for the latter complex was identical with the second oxidation potential for the former complex, 1.49 V (SCE). Kadish et al. formulated the reactions as follows:

$$Mo^{VI}(O)_2(tpp) \rightarrow [Mo^{VI}(O)_2(tpp)]^{+} \tag{18}$$

$$[Mo^{VI}(O)_2(tpp)]^{+} \rightarrow Mo^{V}(O)(ClO_4)(tpp) + O \tag{19}$$

There was no discussion about the fate of the eliminated oxygen atom [57]. The *cis*-dioxo molybdenum(VI) complex first showed an irreversible reduction peak and subsequently two reversible ones at -0.96 V(SCE),

-1.10 V(SCE) and -1.50 V(SCE) respectively, by cyclic voltammetry. Each of these reduction processes is a one-electron process. However, the first reduction process involved two electrons and afforded $Mo^{IV}(O)(tpp)$, clarified by coulometric measurements. The second and third redox pairs observed for $Mo^{VI}(O)_2(tpp)$ were identical with the first and second redox pairs for the corresponding oxomolybdenum(IV) complex [56].

D. PHOTOCHEMISTRY

(i) Niobium porphyrins

The photoreaction of niobium porphyrins was reported in 1985 by Matsuda et al. [23]. The tri-μ-oxo niobium(V) dimer complex with tptp was not reduced under anaerobic irradiation with visible light in benzene, whereas this complex gave a reduced species, $Nb^{IV}(O)(tptp)$, when a small amount of ethanol was added to the solution [24]. The tri-μ-oxo dimer is subject to ligand exchange upon addition of ethanol to form the corresponding mononuclear complex. Although the molecular structure of the monomer species has not been clarified, since this species could not be isolated, its composition has been determined photometrically (eqn. (20)):

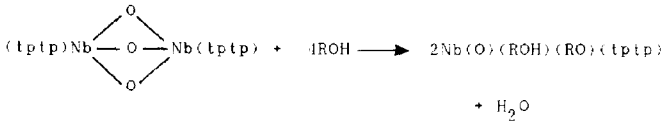

(20)

The above alkoxo complex was subject to photoreduction affording $Nb^{IV}(O)(tptp)$ in a manner similar to the case of the oxoalkoxo molybdenum(V) complexes of porphyrins [58,59] (eqn. (21)):

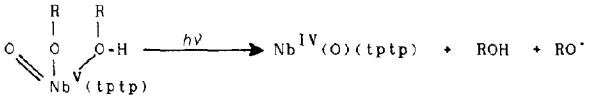

(21)

The product showed visible absorption and ESR spectra identical with those observed for the complex prepared by chemical reduction.

The tri-μ-oxo dimer in benzene upon aerobic irradiation with visible light showed an ESR signal composed of ten hyperfine lines. The A value, 5.08×10^{-4} cm^{-1}, permits evaluation of the odd-electron density at the niobium nucleus, about 3% of that estimated for niobium(IV) porphyrins. The ESR signal presumably originates from a radical species coordinated to the niobium porphyrin. The ESR signal vanished on application of one of the following treatments; deoxygenation of the reaction system; interruption of the irradiation; addition of a radical scavenger such as ethanol. The ESR

signal was attributed to a superoxide complex, $Nb^{V}(O)(OO^{\cdot})(tptp)$. The reaction path during irradiation in benzene was presumed to be as follows. Upon irradiation, one of the bridging Nb–O bonds was cleaved to afford an intramolecular niobium(IV) radical pair (eqn. (22)). Under aerobic conditions, niobium(IV) was attacked by molecular oxygen resulting in formation of two mononuclear species (eqn. (23)), while the intramolecular pair returned to the starting complex by recombination under anaerobic conditions, the reverse of the reaction represented by eqn. (22). The intramolecular pair was formed as an intermediate by intramolecular charge separation and is different from a species obtained by the electrochemical one-electron reduction [18]:

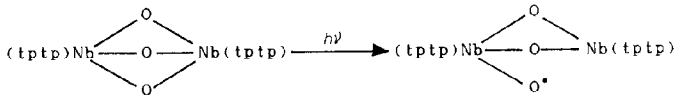

(22)

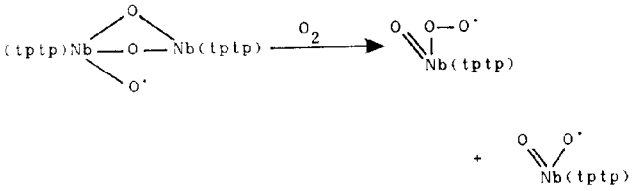

(23)

(ii) Molybdenum porphyrins

The photochemistry of molybdenum porphyrins was reported in 1979 by Ledon and Bonnet [38]. They investigated the reaction of a diperoxomolybdenum(VI) porphyrin, $Mo(O_2)_2(tptp)$, in several solvents such as benzene, toluene, dichloromethane, and THF. $Mo(O_2)_2(tptp)$ gave a complex having a composition consistent with $MoO_2(tptp)$ upon irradiation with visible light under argon. In the light of the splitting of $\nu_{Mo=O}$, the nonequivalence of the phenyl protons and the labile nature of the oxygen atom for exchange, the complex was assumed to have a *cis*-dioxo structure. The molecular geometry was confirmed by X-ray diffraction measurements [37]. The reaction was presumed to take place as follows [58]:

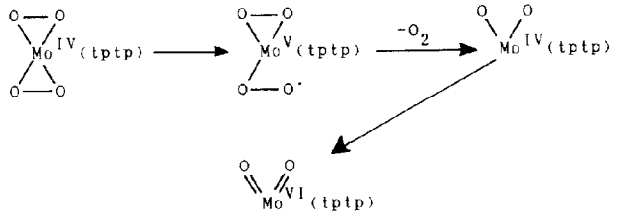

(24)

Ledon and Bonnet reported photoreduction of an oxomethoxo molybdenum(V) porphyrin, $Mo^{V}(O)(OMe)(tpp)$. The complex was reduced in benzene containing 5 vol.% methanol upon aerobic irradiation with visible light [58] (eqn. (25)):

$$Mo^{V}(O)(OMe)(tpp) \rightarrow Mo^{IV}(O)(tpp) + MeO^{\cdot} \tag{25}$$

The reaction was followed by electronic spectroscopy. The radical species generated from the axial ligand was identified by ESR measurements coupled with the spin trapping technique. Reoxidation of the reduced species, $Mo^{IV}(O)(tpp)$, followed second-order kinetics with respect to the reduced complex, indicating that a two-electron reduction process was operative for the molecular oxygen (eqn. (26)):

$$2Mo^{IV}(O)(tpp) + O_2 \xrightarrow{MeOH} 2Mo^{V}(O)(MeO)(tpp) + H_2O_2 \tag{26}$$

Matsuda et al. also observed photoreduction of $Mo^{V}(O)(X)(tptp)$. Complexes having an axial coordination bond of less ionic character were subjected to photo-reduction more readily, while electrochemical reduction proceeded at less negative potentials for complexes having an axial coordination of higher ionic character [59]. The difference in reaction behavior between photochemical and electrochemical reductions must originate from the different cleavage modes of the axial coordination bond. The axial coordination bond was cleaved homolytically in the photoreduction (eqn. (27)), while heterolytic cleavage took place during electrolytic reduction (eqn. (28)):

$$\begin{array}{l} \begin{array}{c} X \\ | \end{array} \\ Mo^{V}(O)(tptp) \end{array} \xrightarrow{h\nu} \left[\begin{array}{l} X^{\cdot} \\ \vdots \\ Mo^{IV}(O)(tptp) \end{array} \right] \searrow Mo^{IV}(O)(tptp) + X^{\cdot} \tag{27}$$

$$\begin{array}{l} \begin{array}{c} X \\ | \end{array} \\ Mo^{V}(O)(tptp) \end{array} \xrightarrow{+e} \left[\begin{array}{l} X^{-} \\ Mo^{IV}(O)(tptp) \end{array} \right]^{-} \searrow Mo^{IV}(O)(tptp) + X^{-} \tag{28}$$

They also examined complexes having axial alkoxo ligands and found that photoreduction of complexes with bulky axial ligands proceeded rather slowly relative to those with smaller ones. This is consistent with an assumption that two steps are involved in the photoreduction. Irradiation with visible light initially gives rise to homolysis of the axial coordination bond resulting in formation of a pair of the reduced metal and a radical species generated from the axial ligand. Two competitive reactions follow

the initial homolysis: a reverse reaction to afford the starting complex by recombination of the pair, and completion of the reduction by the radical species diffusing from the reaction sphere (eqn. (27)).

E. CATALYTIC FUNCTIONS

Since niobium and molybdenum give oxo complexes in their high valence states, the activated transfer of the oxo ligand to substrates may proceed along with the redox reaction of the complexes.

Ledon et al. investigated the reaction of *t*-butyl hydroperoxide with cyclohexene in benzene under anaerobic conditions in the presence of a catalytic amount of an oxomolybdenum complex of tptp at 60–80 °C. They found that epoxidation of cyclohexene proceeded with a selectivity of 85% under the above reaction conditions [60]. *cis*-2-Hexene was more reactive than the *trans* isomer, such reactivity being presumably affected by a steric effect of the porphyrin macrocycle. These authors ruled out participation of the *cis*-dioxomolybdenum(VI) as an active intermediate and alternatively suggested *cis*-$Mo^{IV}(OH)(OO^tBu)$(tpp) to be an active intermediate [61].

Oxygen transfer from the molybdenum porphyrins to substrates was observed in the case of the *cis*-dioxomolybdenum(VI) complexes of tptp by Ledon and Bonnet [39]. The oxidation of a tertiary phosphine by the *cis*-dioxo complex in benzene afforded $Mo^{IV}(O)$(tptp) and the corresponding phosphine oxide (eqn. (29)):

$$Mo^{VI}(O)_2(tptp) + PR_3 \rightarrow Mo^{IV}(O)(tptp) + OPR_3 \quad (29)$$

The reaction rate was primarily affected by steric hindrance.

Another example of oxidation with a *cis*-dioxomolybdenum(VI) porphyrin was reported by the same group [56]. Under anaerobic conditions, secondary alcohols were oxidized to the corresponding ketones with a yield of about 50% based on the complex. The reaction pathway with two one-electron oxidation steps was presumed to be the following:

$$Mo^{VI}(O_2)_2 + R_1R_2CHOH \rightarrow Mo^{VI}(O)(tpp) - R_1R_2C^{\cdot}OH \quad (30)$$

$$Mo^{VI}(O_2)_2 + R_1R_2C^{\cdot}OH \rightarrow Mo^{VI}(O)(tpp) + R_1R_2C{=}O \quad (31)$$

The reaction proceeds as a chain reaction under aerobic conditions, initiated by a ketyl radical and molecular oxygen. The above two examples are stoichiometric reactions under anaerobic conditions. As mentioned in Section D, *cis*-dioxo complexes are highly reactive to oxygen transfer. Regeneration of the starting complexes, however, was not favored. Some highly reactive oxygen sources are required to regenerate the active species in order to drive the catalytic cycle.

The niobium and molybdenum porphyrins were reduced upon irradiation with visible light as mentioned in an earlier section. The reduced species were expected to activate oxidants.

Ledon and Bonnet reported, as mentioned in the preceding section, the photo-assisted reduction of molecular oxygen with $Mo^{V}(O)(OMe)(tpp)$ as a catalyst [58] (eqns. (32)–(34)):

$$Mo^{V}(O)(OMe)(tpp) \rightarrow Mo^{IV}(O)(tpp) + MeO^{\cdot} \quad (32)$$

$$Mo^{IV}(O)(tpp) + 1/2O_2 + MeOH \rightarrow Mo^{V}(O)(OMe)(tpp) + H_2O_2 \quad (33)$$

$$MeO^{\cdot} \rightarrow 1/2MeOH + 1/2HCHO \quad (34)$$

These equations represent photo-assisted catalytic oxidation of methanol.

The reductive activation of atmospheric molecular oxygen with the photochemically reduced niobium porphyrin was reported by Matsuda et al. [23,24]. As mentioned in Section D, the aerobic irradiation of $[\{Nb(tptp)\}_2O_3]$ in benzene afforded two kinds of oxygenated species, $Nb^{V}(O)(O^{\cdot})(tptp)$ and $Nb^{V}(O)(OO^{\cdot})(tptp)$. While the former complex is ESR silent, the latter complex showed a strong and sharp ESR signal composed of ten hyperfine lines. The ESR signal was quenched upon addition of olefins affording exclusively the corresponding epoxides. The reaction proceeded catalytically giving the epoxides in much greater than stoichiometric yield [24]. This is the first example of the exclusive epoxidation of olefins without highly active oxygen sources or reductants (Scheme 4). A similar catalytic reaction was observed with an oxomolybdenum(V) porphyrin [62].

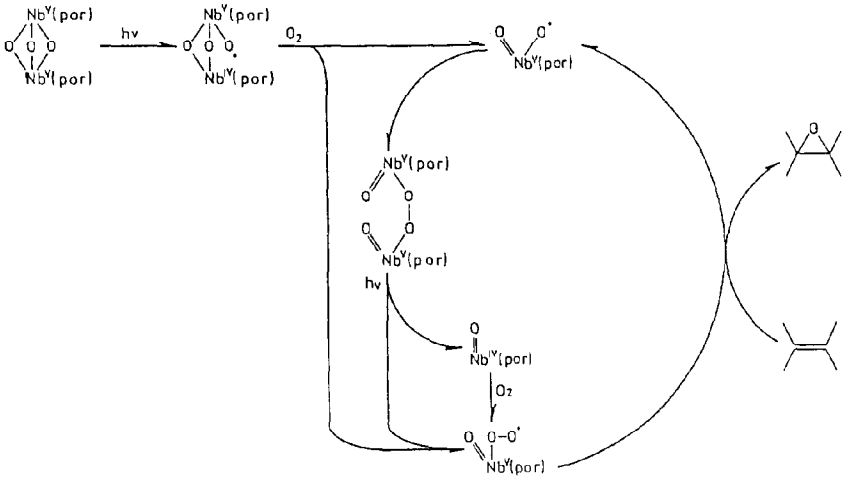

Scheme 4

REFERENCES

1 T.S. Srivastava and E.B. Fleischer, J. Am. Chem. Soc., 92 (1970) 5518.
2 E.B. Fleischer and T.S. Srivastava, Inorg. Chim. Acta, 5 (1971) 151.
3 J.W. Buchler, G. Eikelmann, L. Puppe, K. Rohbock, H.H. Schneehage and D. Weck, Ann. Chem., 745 (1971) 135.
4 J.W. Buchler and K. Rohbock, Inorg. Nucl. Chem. Lett., 8 (1972) 1073.
5 K. Rohbock, Dissertation, Technische Hochschule Aachen, 1972.
6 J.W. Buchler, L. Puppe, K. Rohbock and H.H. Schneehage, Ann. N.Y. Acad. Sci., 206 (1973) 116.
7 J.W. Buchler, L. Puppe, K. Rohbock and H.H. Schneehage, Chem. Ber., 106 (1973) 2710.
8 R. Guilard, B. Fliniaux, B. Maume and P. Fournari, C.R. Seances Acad. Sci., Ser. C, 281 (1975) 461.
9 C. Lecomte, J. Protas, R. Guilard, B. Fliniaux and P. Fournari, J. Chem. Soc., Dalton Trans., (1979) 1306.
10 C. Lecomte, J. Protas, R. Guilard, B. Fliniaux and P. Fournari, J. Chem. Soc., Chem. Commun., (1976) 434.
11 C. Lecomte, J. Protas and R. Guilard, C.R. Acad. Sci., Ser. C, 283 (1976) 397.
12 J.F. Johnson and W.R. Scheidt, Inorg. Chem., 17 (1978) 1280.
13 J.F. Johnson and W.R. Scheidt, J. Am. Chem. Soc., 99 (1977) 294.
14 C. Lecomte, J. Protas, P. Richard, J.M. Barbe and R. Guilard, J. Chem. Soc., Dalton Trans., (1982) 247.
15 M.L.H. Green and J.J.E. Moreau, Inorg. Chim. Acta, 31 (1978) L461.
16 P. Richard and R. Guilard, J. Chem. Soc., Chem. Commun., (1983) 1454.
17 P. Richard and R. Guilard, Nouveau J. Chim., 9 (1985) 119.
18 J.E. Anderson, Y.H. Liu, R. Guilard, J.M. Barbe and K.M. Kadish, Inorg. Chem., 25 (1986) 2250.
19 J.E. Anderson, Y.H. Liu, R. Guilard, J.M. Barbe and K.M. Kadish, Inorg. Chem., 25 (1986) 3786.
20 R. Guilard, P. Richard, M. el Borai and E. Laviron, J. Chem. Soc., Chem. Commun., (1980) 516.
21 Y. Matsuda, T. Goto and Y. Murakami, unpublished result, 1981.
22 Y. Matsuda, S. Yamada, T. Goto and Y. Murakami, Bull. Chem. Soc. Jpn., 54 (1981) 452.
23 Y. Matsuda, S. Sakamoto, T. Takaki and Y. Murakami, Chem. Lett., (1985) 107.
24 Y. Matsuda, S. Sakamoto, H. Koshima and Y. Murakami, J. Am. Chem. Soc., 107 (1985) 6415.
25 H.J. Ledon, M.C. Bonnet, Y. Brigandat and F. Varescon, Inorg. Chem., 19 (1980) 3488.
26 H.J. Ledon, C.R. Acad. Sci., Ser. C, 287 (1978) 59.
27 Y. Matsuda, F. Kubota and Y. Murakami, Chem. Lett., (1977) 1281.
28 H.J. Ledon and B. Mentzen, Inorg. Chim. Acta, 31 (1978) L393.
29 T. Imamura, M. Terui, Y. Takahashi, T. Numatatsu and M. Fujimoto, Chem. Lett., (1980) 89.
30 T. Imamura, T. Numamatsu, M. Terui and M. Fujimoto, Bull. Chem. Soc. Jpn., 54 (1981) 170.
31 T. Diebold, B. Chevrier and R. Weiss, Inorg. Chem., 18 (1979) 1193.
32 R.G. Hayes and W.R. Scheidt, Inorg. Chem., 17 (1978) 1082.
33 Y. Murakami, Y. Matsuda and S. Yamada, Chem. Lett., (1977) 689.
34 T. Imamura, K. Hasegawa, T. Tanaka, W. Nakajima and M. Fujimoto, Bull. Chem. Soc. Jpn., 57 (1984) 194.

35 T. Imamura, T. Tanaka and M. Fujimoto, Inorg. Chem., 24 (1985) 1038.
36 B. Chevrier, T. Diebold and R. Weiss, Inorg. Chim. Acta, 19 (1976) L57.
37 B.F. Mentzen, M.C. Bonnet and H.J. Ledon, Inorg. Chem., 19 (1980) 2061.
38 H.J. Ledon, M.C. Bonnet and J.-Y. Lallemand J. Chem. Soc., Chem. Commun., (1979) 702.
39 H.J. Ledon and M.C. Bonnet, J. Mol. Catal., 7 (1980) 309.
40 K. Hasegawa, T. Imamura and M. Fujimoto, Inorg. Chem., 25 (1986) 2154.
41 T. Imamura, K. Hasegawa and M. Fujimoto, Chem. Lett., (1983) 705.
42 T. Diebold, B. Chevrier and R. Weiss, Angew. Chem., 89 (1977) 819.
43 J. Colin, G. Butler and R. Weiss, Inorg. Chem., 19 (1980) 3828.
44 T. Imamura, M. Takahashi, T. Tanaka, T. Jin, M. Fujimoto, S. Sawamura and M. Katayama, Inorg. Chem., 23 (1984) 3752.
45 A. de Cian, J. Colin, M. Schappacher, L. Ricard and R. Weiss, J. Am. Chem. Soc., 103 (1981) 1850.
46 T. Diebold, M. Schappacher, B. Chevrier and R. Weiss, J. Chem. Soc., Chem. Commun., (1979) 693.
47 J.P. Collman and K.T. Woo, Proc. Natl. Acad. Sci. USA, 81 (1984) 2592.
48 J.-H. Fuhrhop, K.M. Kadish and D.G. Davis, J. Am. Chem. Soc., 95 (1973) 5140.
49 C.M. Newton and D.G. Davis, J. Magn. Reson., 20 (1975) 446.
50 Y. Matsuda and Y. Murakami, in H.F. Barry and P.C.H. Mitchell (Eds.), Proc. Climax 3rd Int. Conf. Chem. Uses Molybdenum, Climax Molybdenum Co., Ann Arbor, MI, 1979, p. 270.
51 Y. Matsuda, S. Yamada and Y. Murakami, Inorg. Chem., 20 (1981) 2239.
52 K.M. Kadish, T. Malinski and H.J. Ledon, Inorg. Chem., 21 (1982) 2982.
53 T. Malinski, P.M. Hanley and K.M. Kadish, Inorg. Chem., 25 (1986) 3229.
54 J. Topich and N. Berger, Inorg. Chim. Acta, 65 (1982) L131.
55 K.M. Kadish, D. Chang, T. Malinski and H.J. Ledon, Inorg. Chem., 22 (1983) 3490.
56 H.J. Ledon, F. Varescon, T. Malinski and K.M. Kadish, Inorg. Chem., 23 (1984) 261.
57 T. Malinski, H.J. Ledon, K.M. Kadish, J. Chem. Soc., Chem. Commun., (1983) 1077.
58 H.J. Ledon, M.C. Bonnet and D. Galland, J. Am. Chem. Soc., 103 (1981) 6209.
59 Y. Matsuda, T. Takaki and Y. Murakami, Bull. Chem. Soc. Jpn., 59 (1986) 1839.
60 H.J. Ledon, P. Durbut and F. Varescon, J. Am. Chem. Soc., 103 (1981) 3601.
61 H.J. Ledon, F. Varescon and P. Durbut, in H.F. Barry and P.C.H. Mitchell (Eds.), Proc. Climax 4th Int., Conf. Chem. Uses Molybdenum, Climax Molybdenum Co., Ann Arbor, MI, 1982, p. 319.
62 Y. Matsuda, K. Nakamura and Y. Murakami, unpublished result, 1985.
63 N. Ohta, W. Scheuermann, K. Nakamoto, Y. Matsuda, S. Yamada and Y. Murakami, Inorg. Chem., 18 (1979) 457.
64 M. Gouterman, L.K. Hanson, G.-E. Khalil, J.W. Buchler, K. Rohbock and D. Dolphin, J. Am. Chem. Soc., 97 (1975) 3142.
65 M.S. Bains and D.G. Davis, Inorg. Chim. Acta, 37 (1979) 53.